

Published in final edited form as:

Dev Biol. 2013 May 15; 377(2): 319–332. doi:10.1016/j.ydbio.2013.03.012.

WAVE/SCAR promotes endocytosis and early endosome morphology in polarized *C. elegans* epithelia

Falshruti B. Patel^a and Martha C. Soto^{a,b}

^aDepartment of Pathology and Laboratory Medicine, UMDNJ – Robert Wood Johnson Medical School, 675 Hoes Lane, Piscataway, NJ 08854

Abstract

Cells can use the force of actin polymerization to drive intracellular transport, but the role of actin in endocytosis is not clear. Studies in single-celled yeast demonstrate the essential role of the branched actin nucleator, Arp2/3, and its activating nucleation promoting factors (NPFs) in the process of invagination from the cell surface through endocytosis. However, some mammalian studies have disputed the need for F-actin and Arp2/3 in Clathrin-Mediated Endocytosis (CME) in multicellular organisms. We investigate the role of Arp2/3 during endocytosis in *C. elegans*, a multicellular organism with polarized epithelia. Arp2/3 and its NPF, WAVE/SCAR, are essential for *C. elegans* embryonic morphogenesis. We show that WAVE/SCAR and Arp2/3 regulate endocytosis and early endosome morphology in diverse tissues of *C. elegans*. Depletion of WAVE/SCAR or Arp2/3, but not of the NPF Wasp, severely disrupts the distribution of molecules proposed to be internalized via CME, and alters the subcellular enrichment of the early endosome regulator RAB-5. Loss of WAVE/SCAR or of the GEFs that regulate RAB-5 results in similar defects in endocytosis in the intestine and coelomocyte cells. This study in a multicellular organism supports an essential role for branched actin regulators in endocytosis, and identifies WAVE/SCAR as a key NPF that promotes Arp2/3 endocytic function in *C. elegans*.

Keywords

morphogenesis; actin nucleation; endocytosis; nucleation promoting factors; early endosomes

INTRODUCTION

The Arp2/3 complex is the only actin nucleator able to promote branched actin formation. The force created by branched actin drives diverse cellular events that require deformation of membranes, from cellular protrusions to membrane trafficking (Reviewed in Chhabra and Higgs, 2007; Pollard, 2007). Arp2/3 is required for endosomal transport in organisms from *Saccharomyces cerevisiae* to mammals, where it contributes to clathrin-mediated endocytosis (CME) (Reviewed in Kaksonen et al., 2006; Toret and Drubin, 2006). While the role of Arp2/3 in CME is well studied in yeast, studies in mammalian cells and in multicellular organisms have been less clear about the CME role of Arp2/3 (Reviewed in Galletta et al., 2010; Liu et al., 2010; Mooren et al., 2012; Robertson et al., 2009). Recent mammalian studies using platinum replica electron microscopy (EM) and dual color total

© 2013 Elsevier Inc. All rights reserved.

^bcorresponding author. PHONE 732-235-4424, FAX 732-235-4825, sotomc@umdnj.edu.

Publisher's Disclaimer: This is a PDF file of an unedited manuscript that has been accepted for publication. As a service to our customers we are providing this early version of the manuscript. The manuscript will undergo copyediting, typesetting, and review of the resulting proof before it is published in its final citable form. Please note that during the production process errors may be discovered which could affect the content, and all legal disclaimers that apply to the journal pertain.

internal reflection fluorescence microscopy (TIR-FM) suggest that the role of branched actin in mammalian cells is more similar to its role in yeast than previously thought, with branched actin present at several steps in CME including clathrin pit invagination, pinching off of pits, and as vesicles move away from the plasma membrane (Collins et al., 2011; Taylor et al., 2011). These studies have generated questions about the types of cells that require Arp2/3 during CME, and how Arp2/3 activation is regulated in such cells.

Arp2/3 and its multiple nucleation-promoting factors (NPFs) are proposed to regulate specific trafficking events. Arp2/3 is a poor actin nucleator until it is activated by one of its NPFs. The multiple Arp2/3 NPFs all contain at least one WCA domain consisting of a G-actin binding WH2 (W) domain and an Arp2/3-binding central/acidic (CA) sequence. WASP (Wiskott-Aldrich Syndrome Protein) and neuronal WASP (N-WASP) are the best studied Arp2/3 NPFs. The yeast Wasp homolog, WASp/Las17, regulates Arp2/3 during CME (Kaksonen et al., 2003); Reviewed in (Mooren et al., 2012). N-WASP is the proposed Arp2/3 NPF during the internalization step of mammalian CME (Benesch et al., 2005; Innocenti et al., 2005; Merrifield et al., 2004), Reviewed in (Firat-Karalar and Welch, 2011). In addition, the Arp2/3 complex and N-WASP have been shown to be sufficient, in an *in vitro* reconstituted system, to drive vesicle scission from tubulated membrane intermediates (Römer et al., 2010). Later steps of endocytic trafficking are thought to require different Arp2/3 NPFs. WASH (WASP and SCAR homology), another Arp2/3 NPF, is thought to regulate early to late-endosome transport, receptor recycling, retromer-mediated endosome-to-Golgi transport and endosome to lysosome transport (Gomez and Billadeau, 2009; Gomez et al., 2012; Harbour et al., 2012). The Arp2/3 NPF WHAMM (WASP homolog associated with actin, membranes and microtubules) facilitates ER-to-Golgi transport (Campellone et al., 2008). The Arp2/3 NPF WAVE (WASP and Verprolin homology), also known as SCAR, has been proposed to regulate vesicle movements in *Drosophila* S2R+ cells (Fricke et al., 2009) and the enrichment of E-cadherin at the plasma membrane in mammalian tissue culture cells (Silva et al., 2009).

Previous work suggested that the Arp2/3 NPF WAVE/SCAR regulates endocytic traffic in *C. elegans* (Giuliani et al., 2009; Shivas and Skop, 2012). *C. elegans* has one homolog of WAVE, rather than three as in mammals, and one homolog each of Wasp and of WASH. The *C. elegans* WAVE complex is composed of five proteins including WVE-1/WAVE/SCAR, GEX-2/ /Sra1/p140/PIR121/CYFIP, GEX-3/NAP1/HEM2/Kette, ABI-1/ABI and NUO-3/HSPC300. Putative null mutations in WVE-1, GEX-2 and GEX-3, and RNAi depletion of ABI-1 have been compared to loss of Wasp or Arp2/3 (Patel et al. 2008). A mutation in WSP-1 has been identified, *wsp-1(gm324)*, that contains a large deletion resulting in no *wsp-1* transcript or protein (Withee et al., 2004). We have proposed that the WAVE complex, rather than WASP, is the major activator of Arp2/3 in developing *C. elegans* embryos, given the similarity of the loss-of-functions phenotypes between WAVE complex and Arp2/3 mutants (Bernadskaya et al., 2011; Patel et al., 2008; Soto et al., 2002). We have further proposed that the Rac homolog CED-10 is the main regulator of the WAVE complex in *C. elegans* embryos, as deletion null alleles of *ced-10* result in 100% embryonic lethality, with most of the embryos dying with similar embryonic morphogenesis phenotypes as embryos missing WAVE complex components (Soto et al., 2002). By contrast, *wsp-1(gm324)* animals are homozygous viable with only a low percent of dead embryos. Another study suggested that F-BAR (Fer/CIP4, Bin, amphiphysin, Rvs) proteins, which bind to membranes and induce their curvature, can recruit the WAVE complex to membranes (Giuliani et al., 2009). In that study the *C. elegans* F-BAR proteins TOCA-1 and TOCA-2 were shown to bind to Wasp and to the WAVE complex component ABI-1 in *C. elegans* and in mammalian cells. Further, the *C. elegans* TOCA proteins, Wasp and WAVE were shown to affect endocytic trafficking into oocytes as well as embryonic development (Giuliani et al., 2009). Studies showing Arp2/3 effects on PAR accumulation in the early *C.*

C. elegans embryo have attributed these effects to Arp2/3 regulation of myosin dynamics (Xiong et al., 2011) and also to Arp2/3 regulation of endosomal dynamics (Shivas and Skop, 2012).

In this study we investigate the endocytosis role of Arp2/3 and two of its NPFs in *C. elegans*, a model organism that has contributed *in vivo* assays of endocytosis and novel genetic insights into the regulation of endocytosis (Fares and Grant, 2002; Grant and Hirsh, 1999). CME regulators in *C. elegans* include clathrin heavy chain (CHC-1), the clathrin adaptor complex AP-2 (including DPY-23, the mu subunit, and APA-2, the alpha subunit) and the large GTPase Dynamin/DYN-1 (Boehm and Bonifacino, 2001; Grant and Hirsh, 1999; Pan et al., 2008). We show here that WAVE/SCAR, rather than Wasp, is the major regulator of Arp2/3 during endocytosis in *C. elegans* adult intestinal epithelia and coelomocytes. Loss of WAVE/SCAR leads to altered transport of a proposed clathrin dependent cargo (GFP::hTfR) in the adult intestine. In addition, the WAVE/SCAR complex is required for the correct morphology of early endosomes (EE) marked by RAB-5 in intestinal epithelia. Experiments in another tissue, the coelomocyte scavenger cells, show that WAVE/SCAR is required for proper endosome morphogenesis and for transport through early endosomes. Similar defects occur when the proteins that help enrich RAB-5 at early endosomes are removed, suggesting branched actin regulators support endocytosis by supporting actin structures that are required to form early endosomes. Our results suggest that WAVE/SCAR works with CME regulators during endocytosis to promote the movement of vesicles away from the plasma membrane. We therefore propose that in the multicellular organism, *C. elegans*, WAVE/SCAR is an essential NPF that supports Arp2/3 endocytic function to promote early endosome morphology.

Materials and Methods

Strains

All strains were cultured as described in Brenner (Brenner, 1974). The following strains were used: FT48 *him-5(e1467); xnIs16 [dlg-1p::dlg-1::gfp; rol-6(d)]*, OX323 *gex-3(zu196)/DnT1; xnIs16 [dlg-1p::dlg-1::gfp; rol-6(d)]*, GS1912 *dpy-20(e1282); arIs37 [myo-3p::ss::gfp dpy-20(+)]*, RT393 *unc-119(ed3); pwIs112 [vha-6p::hTAC::gfp; Cbr-unc-119(+)]*; RT1970 *unc-119(ed3); pwIs90 [vha-6p::gfp::hTfR; Cbunc-119 (+)]*, RT327 *unc-119(ed3); pwIs72 [vha-6p::gfp::rab-5; Cbunc-119(+)]*, RT2287 *unc-119(ed3); [vha-6p::gex-3::gfp; Cbunc-119(+)]*, RT311 *unc-119(ed3); pwIs69 [vha-6p::gfp::rab-11; Cbunc-119(+)]*, RT1103 *unc-119(ed3); pwIs170 [vha-6p::gfp::rab-7; Cbunc-119(+)]*, RT424 *unc-119(ed3); pwIs126 [eea-1p::eea-1::gfp; Cbunc-119(+)]*, DH1336 *bIs34 [rme-8p::rme-8::gfp, rol-6(d)]*, RT67 *rme-6(b1014); bIs34 [rme-8p::rme-8::gfp, rol-6(d)]*, DH1370 *rme-6(b1014)*, VP186 *kbEx138 [aqp-4p::aqp-4::gfp; rol-6(d)]*. The following strains were built for this study: OX439 *wsp-1(gm324); pwIs90 [vha-6p::gfp::hTfR; Cbunc-119(+)]*, OX437 *wsp-1(gm324); dkIs8 [vha-6p::gfp::chc-1; Cbunc-119(+)]*, OX440 *wsp-1(gm324); pwIs72 [vha-6p::gfp::rab-5; Cbunc-119(+)]*, OX567 *rme-6(b1014); pwIs72 [vha-6p::gfp::rab-5; Cbunc-119(+)]*, OX566 *rme-6(b1014); dkIs8 [vha-6p::gfp::chc-1;unc-119(+)]*, OX564 *rme-6(b1014); xnIs16 [dlg-1p::dlg-1::gfp; rol-6(d)]*, OX565 *rme-6(b1014); [vha-6p::gex-3::gfp; Cbunc-119(+)]*, OX559 *rme-6(b1014); pwIs90 [vha-6p::gfp::hTfR; Cbunc-119(+)]*, OX591 *ced-10(n3246); pwIs90 [vha-6p::gfp::hTfR; Cbunc-119(+)]*, OX592 *ced-10(tm597)/nT1-GFP; pwIs90 [vha-6p::gfp::hTfR; Cbunc-119(+)]*, OX420 *pjIs14 [aqp-1p::aqp-1::gfp; rol-6(d)]*.

RNAi by feeding

To examine post-embryonic endocytosis phenotypes we had to remove the WAVE components and *arp-2* via feeding RNAi rather than using existing null mutations. This is

because *gex* mutations are maternal effect lethal. This means that homozygous, zygotic null *gex* animals are rescued by the maternally inherited gene products, and, for example, do not display GFP::hTfR defects. However, their progeny are dead *Gex* embryos that do not hatch (Patel et al., 2008; Soto et al., 2002), so we could not examine the adult endocytosis defects in the next generation.

For feeding RNAi experiments, cDNAs were cloned into L4440 vector and transformed into HT115. Saturated overnight cultures were diluted 1:250 in LB-Amp and grown for 6 hours until the OD600 was close to 1. Bacteria were spun down and resuspended in 100 mg/ml LB Amp and 1mM Isopropyl B-D-1-thiogalactopyranoside (IPTG) was added to the bacteria and plates. For synchronized L1 feeding, hypochlorite treatment was performed on the worms, and the eggs were plated overnight at 15°C for hatching followed by RNAi feeding at 22°C. Efficiency of feeding RNAi for the WAVE/SCAR complex components, *wve-1*, *gex-2*, *gex-3* and *arp-2*, was monitored by counting embryonic lethality for expected levels: 40% for *wve-1* RNAi, 85% for *gex-2* RNAi, 90% lethality for *gex-3* RNAi and 80% for *arp-2* RNAi. RNAi feeding strains for *chc-1*, *rab-5*, *sdpn-1*, *dyn-1*, *apa-2* and *dpy-23* were obtained from the Ahringer library. *rabx-5* and *rabn-5* RNAi strains were provided by B. Grant. For imaging of the adult intestine depleted of *wve-1*, *gex-2*, *gex-3*, *apa-2*, *dpy-23*, *sdpn-1*, *rabx-5* and *rabn-5* synchronized L1s were fed bacteria carrying dsRNA for 60 hours, except for *arp-2*. Since depletion of *arp-2* for 60 hours leads to strong growth defects, *arp-2* was depleted via RNAi food for only 36 hours, which resulted in high levels of embryonic lethality (~60%) but normal intestinal morphology. In the case of *dyn-1*, *chc-1*, *rab-11* and *rab-5* RNAi, feeding L1s led to developmental defects and sterility. Therefore, dsRNA for these genes was fed to L4 staged animals for 24 hours.

RNAi for coelomocyte experiments: Coelomocytes are partially resistant to RNAi (Dang et al., 2004). Therefore for the ssGFP experiments (Figure 1E) synchronized L1s were fed diluted *gex-3* and *arp-2* RNAi bacteria, and were monitored for the expected low percent embryonic lethality. The hatched F1s were transferred after three days onto undiluted *gex-3* and *arp-2* RNAi bacteria. After two days on the stronger RNAi bacteria, the coelomocytes of the gravid adult F1s were imaged. For the RME-8::GFP and EEA-1::GFP experiments (Figure 6) the Figure Legend indicates if the data was collected from the injected animals (P0) or their progeny (F1).

Pulse-chase analysis of coelomocytes

Pulse-chase uptake assay was performed as in Sato *et al.* (Sato et al., 2005). Briefly, 1mg/ml of Texas Red-conjugated BSA (Molecular Probes) was injected into the body cavity in the pharyngeal region of adult worms expressing the integrated *rme-8::gfp* transgene. Injected worms were cultured at room temperature for 10, 30, and 60 minutes, and then intra-cellular trafficking of the dye was halted by placing the plates on ice. The injected worms were then mounted on 3% agarose pads in 1% paraformaldehyde and briefly chilled on ice in a humidifying chamber before imaging of TR-BSA and RME-8::GFP. The center pair of coelomocytes was compared. At least 5 coelomocytes from at least 5 injected worms were analyzed for each time point.

Live imaging of embryos, adult intestines and coelomocytes

Embryos were mounted on 3% agarose pads and images were acquired using the iVision 4.0 software Z-stack program at 1µm intervals. All images acquired on Zeiss Axioskop 2 Plus microscope using a 40x oil objective and a Cooke SensiCam QE camera.

Adults were mounted in 10mM levamisole diluted in M9 buffer on 3% agarose pads. Each pad was imaged within 30 minutes of preparation. All adult intestines were imaged between

the pharynx and the vulva. Z-stack images were acquired at 1 μ m intervals, from the surface of the intestine to the middle of the intestine. Images were captured using Zeiss LSM510 Meta confocal microscope system with 488 nm excitation and spectral fingerprinting function, without interference from auto-fluorescence.

Z-stack images of the coelomocyte were acquired at 1 μ m intervals. The center 4 images were projected and quantified for *myo-3::ssGFP* assay. For *rme-8::gfp* and *eea-1::gfp*, the coelomocytes were quantified from single center focal plane. Image J “line” tool was used to measure the diameter of the endosomes. *myo-3::ssGFP* and *rme-8::gfp* were mounted on 3% agarose pads in 10mM levamisole. However, EEA-1::GFP expression is sensitive to levamisole, therefore the animals were mounted on 10% agarose pad in 0.1 micron polystyrene beads (Polysciences Inc. Cat #00876). Coelomocyte images were captured on Zeiss Axioskop 2 Plus microscope using a 40x oil objective with iVision 4.0 software and a Cooke SensiCam QE camera. At least two independent experiments were performed on different batches of functional RNAi with at least 7 animals per experiment for intestinal as well as coelomocyte imaging.

Adult intestine and embryonic immunostaining

This protocol is modified from Grant and Hirsh, 1999. CME For adult staining 30–40 animals were placed in worm buffer (5% sucrose, 100mM NaCl and 200mM levamisole) on a Poly-L-lysine coated slides and were cut using a 25 gauge needle at the pharynx or tail region such that the intestine and/or gonad are extruded from the adult cuticle. After a 15-minute incubation on dry ice freeze cracking was performed. The adult tissues were fixed in cold methanol for 15 minutes, followed by four one-hour washes in PTB (1% BSA, 1x PBS, 0.1% Tween 20, 0.05% NaN₃, 1mM EDTA) buffer. The slide was then blocked for 30 minutes in 5% fish gelatin diluted in PTB and then incubated in primary (1:200 in PTB) overnight at 4 degrees Celsius. The slides were then washed with PTC Buffer (0.1% BSA, 1x PBS, 0.1% Tween 20, 0.05% NaN₃, 1mM EDTA) buffer four times for an hour each and blocked in PTB buffer for one hour. Preabsorbed secondary antibodies (1:500 in PTB) were added for 2 hours at room temperature and then slides were washed with PTC Buffer four times for an hour each. After the last wash the slides were incubated in PTC buffer overnight at 4 degrees. The slides were mounted in PGND solution (1x PBS containing 80% glycerol, 4% (w/v) N-propyl gallate anti-fade and 0.4mM DAPI). Z-stack images were acquired on Zeiss Axioskop 2 Plus microscope using a 40x oil objective with iVision 4.0 software driving a Cooke SensiCam QE camera. APA-2 antibodies were generous gifts from B. Grant.

Embryos were attached to poly-L-lysine slides and permeabilized by freeze cracking after 15 minutes on dry ice. The slides were fixed for 15 minutes in methanol at -20 degrees, blocked in PBST for 5 minutes, then incubated in primary antibodies at room temperature for 1 hour. α -AJM-1 (mAb MH27, diluted 1:150), and α -LET-413 (Rb, diluted 1:500) were diluted in phosphate-buffered saline (PBS). The slides were washed with PBS and incubated in secondary antibody at room temperature for 2 hours. Slides were mounted in PGND solution. Images were captured on IX81; Olympus equipped with VApo/340 63x 1.15 NA water immersion objective and a Cooke Sensi Cam QE camera.

Lysates for biochemistry

To compare total protein levels in different genetic backgrounds, 100 worms for each genotype were placed in 40ul of RIPA buffer (1M HEPES pH7.2, 5M NaCl, 1M MgCl₂, 100mM EDTA, 5% Sodium Deoxycholate, 10% NP-40 and 10% SDS) containing fresh Protease inhibitors. Then 5X Laemmli buffer was added to the each tube and boiled for 5 minutes at 95°C. Equal amounts of control and RNAi treated samples were loaded on gels

for western blots. Rabbit α -GFP (Abcam 6556) and α -DYN-1 mAb (Iowa Hybridoma Bank) antibodies were used at 1:200 dilution; Rat α -tubulin mAb (Millipore MAB1864) was used at 1:4000 dilution. Secondary antibodies from Jackson Labs, Goat α -Rabbit IgG HRP (Cat# 111-035-0030) and Goat α -mouse IgG HRP (Cat# 115-035-0030), were diluted 1:1000 and Goat Cat# 111-035-0030-Rat IgG HRP (Cat# 112-035-0030) was diluted 1:4000.

Quantitation of immunofluorescence

All quantitation, unless otherwise stated, was done as in papers by the Grant lab (Chen et al., 2006). Average fluorescence intensity was measured with the “circular” selection tool of defined area using Image J. Three randomly selected regions on either apical or basal side were measured per animal. “Mean” intensity was recorded. For GFP::*RAB-7* puncta counts: Object count for maturing (small puncta) and late (larger “ring”-like structure) endosomes were performed in the same defined area. For GFP::*RAB-7* intensity measurements, the Image J “line” tool was used to draw a line through the small or large puncta and the “dynamic profiler” tool was used to measure the average intensity. For the ring-like structures, average intensity from two points of the ring was recorded. At least, six randomly selected puncta and rings per animal were measured. Animals were sampled randomly for the analysis of the various transgenic strains, with one exception. For the quantitation of the effects on GFP::*hTfR* of the three WAVE complex components (*wve-1*, *gex-2* and *gex-3* reduced via RNAi) only animals with large clumps (“affected animals”) were included in the analysis, otherwise the effects showed a trend but were not significant.

Statistical analysis

All statistical analysis was performed using Prism software. All graphs show mean data and standard error of the mean (SEM). Statistical significance for the ungrouped data was established by performing one-way ANOVA (Analysis of Variance) followed by the Tukey post-test. The asterisks (*) indicate p values greater than 0.05.

RESULTS

WAVE/SCAR proteins are needed for endocytosis in two tissues of *C. elegans*.

Most models of clathrin-mediated endocytosis (CME) in multicellular organisms propose a role for the Arp2/3 NPF, Wasp (Reviewed in (Firat-Karalar and Welch, 2011)). To test if WAVE/SCAR or Wasp contributes to CME at apical and basal regions of the *C. elegans* intestine (Figure 1A), we analyzed the distribution of a transgene containing GFP-tagged human transferrin receptor (*hTfR*) (Chen et al., 2006), a protein known to traffic through CME. Reduction of *wve-1*, *gex-2*, or *gex-3* via RNAi (see Materials and Methods) resulted in increased accumulation of GFP::*hTfR* especially at the basal surface, including the formation of large clumps in 52%, 42% and 30% of the animals imaged by confocal microscopy (Figure 1B). Reduction of *wsp-1* via mutation or RNAi did not significantly affect GFP::*hTfR* distribution at apical or basal regions (Figure 1B, B', C'). Reduction of *arp-2* increased GFP::*hTfR* accumulation basally and apically in 100% of the animals examined, a similar effect as loss of known regulators of CME (CHC-1/Clathrin Heavy Chain, DPY-23/ μ subunit of clathrin adaptor AP-2, the APA-2/ α subunit of clathrin adaptor AP-2, or the large GTPase Dynamin/DYN-1) (Figure 1B, B', C, C'). As previously shown, a hypomorphic allele of *ced-10*, *n3246*, alters GFP::*hTfR* distribution (Sun et al., 2012). The *ced-10(tm597)* null allele results in even stronger GFP::*hTfR* accumulation at apical and basal surfaces (Figure 1B, B', C'). These results suggested that Clathrin-Dependent trafficking is strongly affected by the loss of Arp2/3 and its NPF, the WAVE/SCAR complex, although the loss of Arp2/3 leads to stronger defects.

To test if WAVE/SCAR components and Arp2/3 also affect the distribution of transmembrane proteins that are endogenous to the *C. elegans* intestine, we used the basally enriched glycerol-permeable aquaporin channel, AQP-1, and the apically enriched water-permeable channel AQP-4 (Huang et al., 2007). Mammalian homologs of the aquaporins are thought to be localized via clathrin-dependent endocytosis (Katsura et al., 1995; Madrid et al., 2001; Moeller et al., 2010). Loss of *gex-3* or *arp-2* via RNAi resulted in reduced basolateral enrichment of AQP-1 (Figure 1D). Loss of *gex-3* had a noticeable but not statistically significant effect on the ratio of apical to cytoplasmic AQP-4, and the levels of apical AQP-4 were increased. Loss of *arp-2* strongly reduced apical AQP-4 enrichment (Figure 1D). For comparison, depletion of *chc-1* via RNAi resulted in similarly altered accumulation of AQP-1 and AQP-4 at basolateral or apical regions, respectively (Figure 1D). Thus, proper basolateral and apical enrichment of the endogenous *C. elegans* aquaporins, AQP-1::GFP and AQP-4::GFP, respectively, depends on clathrin and on the WAVE/SCAR complex.

To further assess the role of Arp2/3 and WAVE/SCAR in endocytosis we employed the well-established coelomocyte ssGFP uptake assay. This assay measures the ability of GFP fused to signal sequence (ssGFP) and secreted from body-wall muscles (under *myo-3* promoter) to be endocytosed by the coelomocyte scavenger cells (Fares and Greenwald, 2001). Depletion of *gex-3* or *arp-2* via RNAi significantly reduced *myo-3p::ssGFP* accumulation in coelomocytes (Figure 1E). Depletion of *wsp-1* via a deletion mutant had no effect on *myo-3p::ssGFP*. Therefore endocytosis in two tissues, the intestinal epithelium and the coelomocyte cells, requires WAVE/SCAR and Arp2/3.

WAVE/SCAR accumulation is affected by loss of regulators of CME

If WAVE/SCAR proteins contribute to endocytosis, their sub-cellular accumulation may depend on proteins that regulate CME. WAVE/SCAR proteins are enriched at the apical intestine (Patel et al., 2008) (this study, Figure 2A). Loss of CME regulators, including clathrin (*chc-1*), *apa-2*, *dpy-23*, or Dynamin (*dyn-1*), or of the F-BAR genes *toca-2* and *sdpn-1* led to decreased GEX-3::GFP at the apical intestine (Figure 2A, A'). These results suggested that CME regulators, in particular CHC-1 and DYN-1, help recruit the WAVE complex to apical regions. Interestingly, both CHC-1 and DYN-1 have been shown to interact with WAVE complex components (Anitei et al., 2010; Gautier et al., 2011; Tsuboi et al., 2002).

WAVE/SCAR complex regulates the distribution of endocytosis components

The endocytic defects of WAVE/SCAR mutants could reflect WAVE/SCAR requirements at multiple steps, or specific steps in endocytic traffic. To better define the endocytic steps that depend on WAVE/SCAR, we measured the enrichment of molecules that are required for trafficking through specific endocytic compartments including the early endosomes (EE), recycling endosomes (RE) and late endosomes (LE). To monitor effects at EEs we measured the subcellular accumulation of the small GTPase RAB-5. RAB-5 is needed for fusion of endocytic vesicles into early endosomes, and can be visualized using a *gfp::rab-5* transgene (Treich et al., 2004). In wild type intestines GFP::RAB-5 is highly enriched at apical and subapical puncta, with lower accumulation of puncta at the basal regions of the cell. Reduction of *gex-3* or *arp-2* via RNAi led to a significant reduction in the GFP::RAB-5 enrichment at apical and subapical regions, and to significant decrease of basal GFP::RAB-5 in animals depleted of *arp-2*. A null mutation in *wsp-1* had no effect on GFP::RAB-5 distribution (Figure 2B, B'').

Western Blots show that the overall levels of GFP::RAB-5 do not change in *gex-3* or *arp-2* depleted animals (Figure 2B'), so the changes seen are not due to effects of *gex-3* or *arp-2*

on RAB-5 protein levels, but rather to changes in RAB-5 enrichment at presumptive early endosomes (Figure 2B, B'').

Mammalian studies have shown that hTfR joins two populations of early endosomes, one static and one dynamic, both of which can contribute to hTfR recycling. The static early endosomes are RAB-5-associated, heavily dependent on AP-2 and are enriched in hTfR. The dynamic early endosomes are both RAB-5 and RAB-7-associated, AP-2 independent, and can mature into late endosomes (Reviewed in Mayle et al., 2012). Since the intensity of RAB-5-positive endosomes decreased in WAVE/SCAR mutants (Figure 2B), we wanted to monitor effects on both recycling endosomes and late endosomes. To monitor WAVE/SCAR effects on recycling endosomes we measured the accumulation of GFP::RAB-11 (Chen et al., 2006). In wild type intestines GFP::RAB-11 is highly enriched at apical and subapical puncta, with lower accumulation at the basal regions of the cell. Reduction of *gex-3* or *arp-2* via RNAi led to a significant reduction in the apical and subapical accumulation of GFP::RAB-11, while a null mutation in *wsp-1* had no effect (Figure 2C). To monitor WAVE/SCAR effects on late endosomes we monitored GFP::RAB-7 (Hermann et al., 2005). In wild type intestines GFP::RAB-7 localized to small puncta (putative maturing endosomes) and to larger late endosomes (Römer et al., 2010) throughout the cytoplasm with enrichment at cytoplasmic basal regions (Figure 2D). Reduction of *gex-3* or *arp-2* via RNAi led to reduced number of small puncta enriched in GFP::RAB-7 and an increase in the number of large puncta (Figure 2D). The large puncta were easy to detect in animals depleted of *gex-3*, as overall GFP::RAB-7 intensity levels were elevated. In contrast, the large puncta were difficult to detect in *arp-2* depleted animals as the overall GFP::RAB-7 intensity levels decreased (Figure 2D). We conclude from these results that WAVE/SCAR contributes significantly to the early endosomes enriched in RAB-5. There are also effects on recycling endosomes enriched in RAB-11, and late endosomes enriched in RAB-7, that may be associated with the effects on RAB-5. Interestingly, loss of *rab-5* via RNAi led to similar effects on GFP::RAB-11 and GFP::RAB-7, most similar to the loss of *arp-2* (Figure 2C, D).

Endocytic molecules and WAVE/SCAR regulate morphogenesis in embryonic epithelia

The finding that WAVE/SCAR proteins contribute to endocytosis led us to ask if defects in trafficking could contribute to the Gex embryonic morphogenesis defects and lethality. WAVE/SCAR mutants have distinctive epithelial morphogenesis defects including a wider intestinal lumen and failure in epidermal cell migrations. These morphogenesis defects are accompanied by correct cell fate and tissue differentiation (Patel et al., 2008; Soto et al., 2002). Gex mutants also establish clear apical and basal epithelial compartments (Figure 3A), suggesting Gex defects are not due to overall defects in polarity. Using the DLG-1::GFP transgene (Totong et al., 2007) to visualize the epithelial tissues we found that endocytosis mutants, including *chc-1*, *dyn-1* and *rab-5*, showed intestinal lumen expansion, and failures in epidermal enclosure strikingly similar to those seen in Gex mutants (Figure 3B). In contrast to loss of WAVE/SCAR, which results in 100% of the embryos dying with the Gex morphogenesis phenotype, only a subset of the embryos missing endocytosis regulators showed the Gex phenotype. This difference in penetrance of the Gex phenotype resulted from the fact that only embryos that made it through early embryogenesis and differentiated tissues were scored for morphogenesis phenotypes. Since the “Early Arrest” and “Morphogenesis” phenotypes are mutually exclusive, we probably undercounted the contribution of some endocytosis genes to morphogenesis since we could not include embryos that failed to undergo differentiation. For example, loss of *rab-5* often resulted in “Early Arrest” due to defects in events that occurred before morphogenetic movements began (Hyenne et al., 2012; Nakayama et al., 2009) (Figure 3B). Thus, endocytosis appears

to play a role in epithelial morphogenesis in both the epidermis and intestine during embryonic development.

WAVE/SCAR localization relative to cellular membranes and endocytosis proteins

If the WAVE/SCAR complex is promoting endocytosis, particularly at the early endosomes, we would expect WAVE proteins to be enriched subcellularly at either the plasma membrane or at early endosomes, or at both places. The WAVE complex localizes to the apical intestine (Patel et al., 2008), but the subcellular distribution in this tissue is not known. The GEX-3::GFP transgene was enriched apically, where it overlapped the terminal web, (MH33 antibody to IFB-2, (Bossinger et al., 2004; Francis and Waterston, 1985)) and was enriched basally, where it overlapped with the LET-413/Scribble (Legouis et al., 2000) plasma membrane-enriched protein (Figure 4A). Therefore GEX-3::GFP is enriched at or near membranes where endocytosis occurs.

If the WAVE/SCAR complex regulates endocytosis, it should be enriched at similar regions as endocytosis regulators. GFP::CHC-1 localizes to the apical intestine, where it regulates lumen morphogenesis (Zhang et al., 2012). Confocal images demonstrated that GFP::CHC-1 has a similar apical enrichment as GEX-3::GFP, where it colocalized partially with the apical terminal web (α -IFB-2, Figure 4A) and with GEX-3::GFP (Figure 4B). APA-2 was enriched at the basal plasma membrane, as shown by its colocalization with PH::GFP (Figure 4B). APA-2 was also enriched at regions where some GEX-3::GFP and some GFP::RAB-5-positive puncta are found (Figure 4B). Therefore GEX-3::GFP is enriched subcellularly at the plasma membrane, and at puncta that are also enriched for CHC-1, APA-2 and RAB-5.

WAVE/SCAR effects on subcellular distribution of GFP::hTfR

To determine where GFP::hTfR accumulates when WAVE/SCAR components are reduced, we first asked where GFP::hTfR is normally found. In wild type animals double staining of the GFP::hTfR transgenic strain with antibodies to GFP and to individual regulators of CME showed that GFP::hTfR has a similar localization pattern as puncta enriched for APA-2 and RAB-5. These results suggested that normally some hTfR is found at the plasma membrane, and some at early endosomes. When we depleted the WAVE/SCAR component *gex-3* by RNAi, there was a shift in the accumulation of GFP::hTfR with increased accumulation at the region enriched in APA-2. In addition, there was less hTfR at the region enriched in RAB-5-positive puncta (Figure 4C). The shift of GFP::hTfR in *gex-3* depleted animals away from EEs to the APA-2-positive puncta at the presumptive cell surface suggested GEX-3 is needed for GFP::hTfR to leave the cell surface and move to early endosomes.

WAVE/SCAR affects early endosomes in the coelomocytes

If WAVE/SCAR has a general role in the regulation of early endosome morphology, we would expect it to show similar defects at other tissues besides the intestine. We therefore analyzed another tissue well characterized for its endocytic role, the coelomocyte scavenger cells (Fares and Grant, 2002; Fares and Greenwald, 2001; Sato et al., 2005). We had noted decreased uptake into coelomocytes in animals depleted of *gex-3* or *arp-2* (Figure 1E). The early endosomes in the coelomocytes are large and easy to image, for example using the RME-8::GFP transgene. RME-8 function is required for transport through endosomes in coelomocytes (Zhang et al., 2001). The coelomocytes are partially resistant to RNAi (Dang et al., 2004), so we report the results here for *gex-3* RNAi animals in the 2nd generation on RNAi food (F1s), and for *arp-2* animals in the first generation (Materials and Methods). These RNAi results are likely underestimating the role of *gex-3* and *arp-2* in coelomocytes. Since the early endosomes enriched in RME-8::GFP vary in size, we measured the number of small endosomes (under 2 μ m in diameter) and the number of large endosomes (over 2

µm in diameter). Reduction of *gex-3* or of *arp-2* via RNAi resulted in nearly normal numbers of the smaller RME-8-positive endosomes, but a significant decrease in the number of the larger RME-8-positive endosomes (Figure 5A, A'). In addition, in 23% of the *gex-3* animals and 20% of the *arp-2* animals, the larger endosomes were completely lost, as occurs in *rme-6* mutants (Figure 5A). For comparison, loss of RME-6, a GEF for RAB-5 that is required for proper formation of early endosomes in coelomocytes, results in small RME-8::GFP-positive endosomes and almost no large endosomes (Figure 5A, A'). These results suggested that early endosomes are forming in animals depleted of *gex-3* and *arp-2*, but are not maturing normally into large RME-8::GFP-positive endosomes. To further explore what steps in early endosome function are being affected, we also examined the accumulation of EEA-1::GFP, which is also enriched at early endosomes in the coelomocytes (Sato et al., 2005; Shi et al., 2009). EEA1 is a RAB-5 effector protein that regulates early endosome docking and fusion (Christoforidis et al., 1999; Simonsen et al., 1998). *gex-3* and *arp-2* depleted animals accumulated significantly fewer large EEA-1::GFP-positive endosomes (Figure 5B, B'). This result supported the finding that WAVE/SCAR regulates the maturation of early endosomes in coelomocytes.

If WAVE/SCAR is required for early endosome maturation, then loss of WAVE/SCAR should affect transport through the early endosomes. We therefore tested transport through the RME-8-positive endosomes in *gex-3* and *arp-2* animals by injecting Texas Red-BSA (TR-BSA) into the body cavity of animals expressing RME-8::GFP and waiting 10, 30 or 60 minutes before monitoring if TR-BSA has arrived at, or left the endosomes. For comparison, wild type animals show TR-BSA accumulation within the RME-8::GFP-positive endosomes after 10 minutes, and transport out of these endosomes by 30 minutes. *rme-6* mutants display strong delays in transport through these endosomes, requiring over an hour (Sato et al., 2005; Figure 5C). Depletion of *gex-3* or *arp-2* via RNAi led to a significant delays in TR-BSA exit from the RME-8::GFP-positive endosomes (Figure 5C). At 30 minutes TR-BSA had exited the RME-8-positive endosomes in only 2/5 *arp-2* animals and 4/8 *gex-3* RNAi animals. At 60 minutes TR-BSA had exited the RME-8-positive endosomes in 5/5 *arp-2* animals and in 4/7 *gex-3* animals. We conclude that WAVE/SCAR is required for efficient transport through the RME-8-positive early endosomes.

To test if the RAB-5 GEF *rme-6* works at a similar step as WAVE/SCAR during endocytosis in another tissue, the intestine, we monitored GFP::hTfR accumulation in *rme-6* mutants, and in doubles with two genes *rme-6* is redundant with, the RAB-5 GEF, *rabx-5*, and the RAB-5 effector, *rabn-5* (Sato et al., 2005). We found that single mutants had mild GFP::hTfR defects, while all double mutants for these RAB-5 interactors led to dramatic loss of GFP::hTfR transport in the intestine (Figure 1B, lower panels, B'), with GFP::hTfR clumping defects as strong as loss of CHC-1 or ARP-2. We also monitored the effects of *rme-6* and other RAB-5 interactors on morphogenesis, and noted that the *rme-6*; *rabx-5(RNAi)* double mutant resulted in high levels of Gex-like morphogenesis defects (Figure 3B). Altogether these results suggested that WAVE/SCAR and the RAB-5 GEFs have shared roles in endocytosis, and that this role involves promoting the maturation of early endosomes and transport through the early endosomes.

DISCUSSION

Studies using tissue culture cells have identified Wasp and N-Wasp as the NPFs responsible for Arp2/3 activation during the invagination steps of CME (Benesch et al., 2005; Innocenti et al., 2005; Merrifield et al., 2004). The results shown here, based on the multicellular organism *C. elegans*, show that WAVE/SCAR is an essential NPF for Arp2/3 during endocytosis. The developmental role of Arp2/3 in membrane trafficking is well supported by studies showing that *Drosophila* and nematodes developing in the absence of the F-BAR

proteins CIP4, TOCA-1 and TOCA-2 are defective in morphogenesis. Since CIP4 and TOCAs bind directly to Wasp, it has been proposed that the effects of Arp2/3 on endocytic trafficking are likely due to the role of Wasp (Leibfried et al., 2008). However, TOCAs can also bind to the WAVE complex through its ABI-1 subunit (Fricke et al., 2009; Giuliani et al., 2009). In addition, the loss of the WAVE complex has as strong or stronger effects on trafficking events in flies and nematodes (Fricke et al., 2009; Giuliani et al., 2009; this study). In this study we compared the role of the Arp2/3 NPFs Wasp and WAVE complex and found stronger phenotypes for WAVE in endocytosis. Further, we characterized the steps in endocytic traffic that require WAVE, and discovered an important role of the WAVE complex regulating the subcellular enrichment of the early endosome regulator RAB-5, and the maturation of early endosomes.

The role of actin during mammalian CME is still controversial. The drug treatments used to depolymerize actin in some mammalian studies may explain this. Collins and colleagues (Collins et al., 2011) found that at the drug doses typically used in those studies, not all actin is depolymerized. In addition, one study suggested that two distinct clathrin structures exist, and only one type of clathrin structure, the clathrin plaques, but not the clathrin pits, requires actin (Saffarian et al., 2009). Others have suggested that changes in cortical tension contribute to clathrin-mediated endocytosis (Liu et al., 2010). Further, actin dynamics have been proposed to counteract membrane tension to promote CME (Boulant et al., 2011). These studies suggested that the plasma membrane of some tissue culture cells is simply not under the same level of tension as that of yeast cells, or perhaps as that of cells in a multicellular organism. Therefore branched actin, which is proposed to provide force for membrane deformation, may not be as important for CME in some tissue culture cells (Mooren et al., 2012). The role of WAVE and WAVE/SCAR components in endocytosis in other organisms may have been similarly missed. One mammalian study (Innocenti et al., 2005) reported that depletion of two WAVE/SCAR components, Nap1/GEX-3 and ABI/ABI-1, increased EGFR surface accumulation, a clathrin-dependent process. In addition, it is possible that for tissue culture cells loss of Clathrin will cause a much more penetrant effect on transferrin endocytosis than loss of the WAVE/SCAR complex components, perhaps due to the low levels of tension at the plasma membrane. This could explain why depletion of CYFIP/GEX-2 (Anitei et al., 2010) and Nap1/GEX-3 (Gautier et al., 2011) in tissue culture cells via RNAi did not affect transferrin uptake relative to clathrin depletion. In our *in vivo* system, the effects on GFP::hTfR distribution were as strong when Arp2/3 was depleted as when Clathrin, APA-2/a-adaptin or Dynamin were removed (Figure 1).

A model for the role of WAVE/SCAR in endocytosis regulation

Our results suggest WAVE/SCAR may support endocytosis at two steps: WAVE/SCAR may promote endocytic movement away from the plasma membrane, and the maturation of a subset of early endosomes (Figure 6). The increased GFP::hTfR accumulation at APA-2-positive regions seen in WAVE/SCAR mutants (Figure 4C) suggested WAVE/SCAR normally promotes transport of cargo away from the plasma membrane. Therefore WAVE/SCAR may be recruited to the plasma membrane to promote early events in CME, including membrane tubulation, vesicle scission, and movement of the vesicle away from the membrane. To better understand this function of WAVE/SCAR, it will be necessary to identify the molecules that recruit WAVE/SCAR to the plasma membrane. Several candidates exist, including Dynamin/DYN-1, which was identified in a screen for *C. elegans* GEX-3 yeast two-hybrid interactors (Tsuboi et al., 2002). In addition, Clathrin Heavy Chain binds to CYFIP, a GEX-2 homolog and component of the WAVE Complex, in mammalian studies (Anitei et al., 2010; Baust et al., 2006) while other studies show CHC-1 can also bind to other WAVE/SCAR complex components including WVE-1 and ABI-1 (Gautier et al., 2011). Finally, the WAVE/SCAR component ABI-1 binds to the F-BAR proteins

TOCA/CIP4 in *C. elegans* and *Drosophila*, and mammalian cells (Fricke et al., 2009; Giuliani et al., 2009). We have observed that the F-BAR proteins SDPN-1 and TOCA-2 have roles in embryonic morphogenesis, in localizing different CME regulators, and in enriching GEX-3 apically (Giuliani et al., 2009; Figure 2A). A more thorough analysis of the seven *C. elegans* F-BAR proteins is needed to determine which F-BARs are required to recruit Arp2/3 and the WAVE complex during CME.

Our results suggest that WAVE/SCAR and Arp2/3 may promote the formation of a subset of early endosomes derived from the plasma membrane. In mammalian studies hTfR is known to join two populations of early endosomes, one static and one dynamic, which contribute to hTfR recycling. The static early endosomes are RAB5-associated, heavily dependent on AP-2 and are enriched in hTfR. The dynamic early endosomes are both RAB5 and RAB7-associated, AP-2 independent, and can mature into late endosomes (Reviewed in Mayle et al., 2012). While further studies are needed to test if *C. elegans* also has populations of static and dynamic early endosomes, using the model of these two populations of early endosomes helps to put our results into a framework. We find that the intensity of RAB-5-positive endosomes decreases in WAVE/SCAR mutants (Figure 2B), while the intensity of APA-2-associated hTfR increases (Figure 4C). In addition, loss of GEX-3 reduces the apical enrichment of RAB-11, a regulator of recycling endosomes, and shifts the enrichment of RAB-7 from the small putative maturing endosomes to the larger late endosomes (Figure 2C, D). These results suggest that decreased slow transport from the static early endosomes may contribute to decreased recycling. The increase in the number of the large RAB-7 puncta may indicate that since transport to recycling endosomes is decreased, additional transport to the late endosomes occurs (Figure 6). Therefore WAVE/SCAR, possibly in collaboration with the RAB-5 GEFs and effectors, may help APA-2 form the static population of early endosomes. To explain the strong GFP::hTfR basal accumulation phenotype in animals depleted of *arp-2* or WAVE/SCAR components, we therefore propose that two endocytic steps may be defective in the absence of WAVE/SCAR: transport from the plasma membrane to early endosomes, and the process that creates the static EEs, which contribute to recycling endosome formation. Since loss of *arp-2* had much stronger effects than loss of WAVE components, like *gex-3*, in most of the endocytosis assays we tested, our results leave open the possibility that additional NPFs are acting to activate *arp-2* during these steps in endocytosis.

The role of WAVE/SCAR in trafficking at apical and basal membranes

Recent studies in *C. elegans* have identified the clathrin adaptor AP-1 as an important regulator of polarity maintenance in the intestine with effects on both apical and basolateral transmembrane proteins. Loss of AP-1 subunits resulted in ectopic lumen formation. Michaux and colleagues demonstrated that these effects resulted from changes in the apical enrichment of molecules important for the apical epithelia including the small GTPase CDC-42 and PAR-6 (Shafaq-Zadah et al., 2012). Göbel and colleagues discovered a role for clathrin and AP-1 not just in maintenance of the apical domain due to effects on the apical PAR complex proteins and ERM-1, but also found evidence that AP-1 regulates an apically directed transport route that converges with a sphingolipid-dependent apical trafficking pathway to regulate the apical regions of the intestinal epithelia (Zhang et al., 2012).

When we compared the loss of WAVE/SCAR or Arp2/3 to the loss of AP-1, we did not see similar defects. For example, we have never observed ectopic apical lumens. We have also documented that apically enriched proteins, including ERM-1, are enriched at the apical membrane of WAVE and Arp2/3 depleted animals (Bernadskaya et al., 2011). However, WAVE/SCAR components and *arp-2* are involved in the regulation of both apical and basolateral transmembrane proteins. Using transgenes to aquaporin channels endogenous to the *C. elegans* intestine, we detected decreased enrichment of both apical and basolaterally

enriched aquaporins when *gex-3*, *arp-2*, or *chc-1* were depleted (Figure 1D). These results show that while overall apical/basal polarity is established (Figure 3A), the maintenance of transmembrane proteins at their correct apical or basolateral regions requires WAVE/SCAR and Arp2/3. Our results further suggest that another clathrin adapter, AP-2, promotes endocytosis through WAVE/SCAR (Figure 4).

Do WAVE/SCAR and CED-10/Rac1 have a similar role in endocytosis?

A recent *C. elegans* study has proposed that a protein in the WAVE/SCAR pathway, CED-10/Rac1, regulates basolateral endocytic recycling by down-regulating RAB-5 in the intestine, with similar effects on RAB-5 as loss of the RAB-5 GAP protein, TBC-2 (Sun et al., 2012). If CED-10/Rac1 and WAVE work together in endosomal transport, as they do during embryonic morphogenesis, we would expect similar defects when they are removed, but this is not always the case. Loss of *ced-10* results in GFP::hTfR defects, including increased accumulation at basal and apical regions (Sun et al., 2012), just as is seen in WAVE mutants (Figure 1B, C), so all appear to regulate CME. In addition, both CED-10 and WAVE/SCAR affect molecules important for endocytic recycling (Sun et al., 2012, this manuscript, Figure 2C). However, while loss of WAVE components resulted in decreased GFP::RAB-5 (Figure 2B, B''), the hypomorphic allele of *ced-10* resulted in increased GFP::RAB-5, suggesting activated CED-10 normally promotes RAB-5 turnover (Sun et al., 2012). In addition, WAVE mutants do not share other RAB-5 GAP phenotypes of TBC-2, like increased ssGFP accumulation (Chotard et al., 2012). Instead, loss of WAVE components and *arp-2* results in decreased ssGFP accumulation (Figure 1E). There are two simple ways to explain this discrepancy. First, it is possible that CED-10/Rac1 acts only to regulate recycling, while the WAVE/SCAR complex is recruited and activated during other steps in endocytosis by other molecules. The second possibility is that full loss of CED-10 would result in similar effects on RAB-5 as what was shown here, since the use of *ced-10* hypomorphs has a history of giving confusing results (Kinchen et al., 2005). To address this idea, we assayed the effect of a *ced-10* null allele, *tm597*, on GFP::hTfR. Even though there is maternal rescue in these animals, the effect of the null allele on GFP::hTfR is much stronger than that of the hypomorph (Figure 1B, B', C'). Additional assays of early endosome morphogenesis in coelomocytes and intestines in null *ced-10* mutants will help address this question.

Conclusion

Our studies connect WAVE/SCAR to endocytosis in *C. elegans* (Figures 1–5). They also indicate that endocytosis regulators may contribute to epidermal morphogenesis (Figure 3B). The connection between actin regulators and endocytosis has been suggested by mammalian studies that proposed that activation of Rac1 requires transport to endosomes (Palamidessi et al., 2008). These studies suggested endocytosis is needed to help activate actin nucleation. The results shown here raise a new possibility, that actin nucleation is activating endocytosis at early endosomes. While we have not yet been able to show a biochemical connection between the RAB-5 GEFs and WAVE/SCAR, loss of the RAB-5 GEFs reduces apical GEX-3::GFP accumulation (Figure 2A), and loss of WAVE/SCAR reduces GFP::RAB-5 accumulation (Figure 2B). Therefore the RAB-5 GEFs may help recruit WAVE/SCAR so that WAVE-dependent actin nucleation can create branched actin structures necessary for the GTPase RAB-5 to assemble at early endosomes and promote their maturation.

Acknowledgments

We would like to thank the NCCR-funded *Caenorhabditis* Genetics Center, Hanna Fares, Todd Lamitina and Barth Grant, for strains, the NICHD-funded University of Iowa Hybridoma Bank for the antibodies to DYN-1, IFB-2 and ERM-1, Jon Audhya for antibodies to RAB-5, Renaud Legouis for the antibody to LET-413, Zhiyong Bai and Barth Grant for the RT2287 strain, and Barth Grant for antibodies to CHC-1, RME-2 and APA-2, and for advice on

endocytosis assays and staining of adult intestines. Thanks to Dr. Carolina Wahlby at CellProfiler (Broad Institute) for advice on quantitation. We thank Barth Grant, Loren Runnels and two anonymous reviewers for helpful suggestions on the manuscript. This research was funded by grants from the NIH (GM081670) and NSF (0641123) to M.C.S.

References

- Anitei M, Stange C, Parshina I, Baust T, Schenck A, Raposo G, Kirchhausen T, Hoflack B. Protein complexes containing CYFIP/Sra/PIR121 coordinate Arf1 and Rac1 signalling during clathrin-AP-1-coated carrier biogenesis at the TGN. *Nat Cell Biol.* 2010; 12:330–340. [PubMed: 20228810]
- Baust T, Czupalla C, Krause E, Bourel-Bonnet L, Hoflack B. Proteomic analysis of adaptor protein 1A coats selectively assembled on liposomes. *Proceedings of the National Academy of Sciences of the United States of America.* 2006; 103:3159–3164. [PubMed: 16492770]
- Benesch S, Polo S, Lai FPL, Anderson KI, Stradal TEB, Wehland J, Rottner K. N-WASP deficiency impairs EGF internalization and actin assembly at clathrin-coated pits. *Journal of Cell Science.* 2005; 118:3103–3115. [PubMed: 15985465]
- Bernadskaya YY, Patel FB, Hsu HT, Soto MC. Arp2/3 promotes junction formation and maintenance in the *Caenorhabditis elegans* intestine by regulating membrane association of apical proteins. *Molecular Biology of the Cell.* 2011; 22:2886–2899. [PubMed: 21697505]
- Boehm M, Bonifacino JS. Adaptins: The Final Reckoning. *Molecular Biology of the Cell.* 2001; 12:2907–2920. [PubMed: 11598180]
- Bossinger O, Fukushige T, Claeys M, Borgonie G, McGhee JD. The apical disposition of the *Caenorhabditis elegans* intestinal terminal web is maintained by LET-413. *Developmental Biology.* 2004; 268:448–456. [PubMed: 15063180]
- Boulant S, Kural C, Zeeh JC, Ubelmann F, Kirchhausen T. Actin dynamics counteract membrane tension during clathrin-mediated endocytosis. *Nat Cell Biol.* 2011; 13:1124–1131. [PubMed: 21841790]
- Brenner S. THE GENETICS OF CAENORHABDITIS ELEGANS. *Genetics.* 1974; 77:71–94. [PubMed: 4366476]
- Campellone KG, Webb NJ, Znameroski EA, Welch MD. WHAMM is an Arp2/3 complex activator that binds microtubules and functions in ER to Golgi transport. *Cell.* 2008; 134:148–161. [PubMed: 18614018]
- Chen CCH, Schweinsberg PJ, Vashist S, Mareiniss DP, Lambie EJ, Grant BD. RAB-10 is required for endocytic recycling in the *Caenorhabditis elegans* intestine. *Molecular Biology of the Cell.* 2006; 17:1286–1297. [PubMed: 16394106]
- Chhabra ES, Higgs HN. The many faces of actin: matching assembly factors with cellular structures. *Nat Cell Biol.* 2007; 9:1110–1121. [PubMed: 17909522]
- Chotard L, Mishra AK, Sylvain MA, Tuck S, Lambright DG, Rocheleau CE. TBC-2 Regulates RAB-5/RAB-7-mediated Endosomal Trafficking in *Caenorhabditis elegans*. *Molecular Biology of the Cell.* 2010; 21:2285–2296. [PubMed: 20462958]
- Christoforidis S, McBride HM, Burgoyne RD, Zerial M. The Rab5 effector EEA1 is a core component of endosome docking. *Nature.* 1999; 397:621–625. [PubMed: 10050856]
- Collins A, Warrington A, Taylor Kenneth A, Svitkina T. Structural Organization of the Actin Cytoskeleton at Sites of Clathrin-Mediated Endocytosis. *Current Biology.* 2011; 21:1167–1175. [PubMed: 21723126]
- Dang H, Li Z, Skolnik EY, Fares H. Disease-related Myotubularins Function in Endocytic Traffic in *Caenorhabditis elegans*. *Molecular Biology of the Cell.* 2004; 15:189–196. [PubMed: 14565969]
- Fares H, Grant B. Deciphering Endocytosis in *Caenorhabditis elegans*. *Traffic.* 2002; 3:11–19. [PubMed: 11872138]
- Fares H, Greenwald I. Genetic Analysis of Endocytosis in *Caenorhabditis elegans*: Coelomocyte Uptake Defective Mutants. *Genetics.* 2001; 159:133–145. [PubMed: 11560892]
- Firat-Karalar EN, Welch MD. New mechanisms and functions of actin nucleation. *Current Opinion in Cell Biology.* 2011; 23:4–13.

- Francis GR, Waterston RH. Muscle organization in *Caenorhabditis elegans*: localization of proteins implicated in thin filament attachment and I-band organization. *The Journal of Cell Biology*. 1985; 101:1532–1549.
- Fricke R, Gohl C, Dharmalingam E, Grevelhörster A, Zahedi B, Harden N, Kessels M, Qualmann B, Bogdan S. *Drosophila* Cip4/Toca-1 Integrates Membrane Trafficking and Actin Dynamics through WASP and SCAR/WAVE. *Current Biology*. 2009; 19:1429–1437.
- Galletta BJ, Mooren OL, Cooper JA. Actin dynamics and endocytosis in yeast and mammals. *Current Opinion in Biotechnology*. 2010; 21:604–610.
- Gautier JJ, Lomakina ME, Bouslama-Oueghlani L, Derivery E, Beilinson H, Faigle W, Loew D, Louvard D, Echard A, Alexandrova AY, Baum B, Gautreau A. Clathrin is required for Scar/Wave-mediated lamellipodium formation. *Journal of Cell Science*. 2011; 124:3414–3427. [PubMed: 22010197]
- Giuliani C, Troglio F, Bai Z, Patel FB, Zucconi A, Malabarba MG, Disanza A, Stradal TB, Cassata G, Confalonieri S, Hardin JD, Soto MC, Grant BD, Scita G. Requirements for F-BAR Proteins TOCA-1 and TOCA-2 in Actin Dynamics and Membrane Trafficking during *Caenorhabditis elegans* Oocyte Growth and Embryonic Epidermal Morphogenesis. *PLoS Genet*. 2009; 5:e1000675. [PubMed: 19798448]
- Gomez TS, Billadeau DD. A FAM21-Containing WASH Complex Regulates Retromer-Dependent Sorting. *Developmental Cell*. 2009; 17:699–711.
- Gomez TS, Gorman JA, Artal-Martinez NA, Koenig AO, Billadeau DD. Trafficking Defects in WASH Knockout Fibroblasts Originate from Collapsed Endosomal and Lysosomal Networks. *Molecular Biology of the Cell*. 2012; 23(16):3215–28. [PubMed: 22718907]
- Grant B, Hirsh D. Receptor-mediated Endocytosis in the *Caenorhabditis elegans* Oocyte. *Molecular Biology of the Cell*. 1999; 10:4311–4326. [PubMed: 10588660]
- Harbour ME, Breusegem SY, Seaman MNJ. Recruitment of the endosomal WASH complex is mediated by the extended ‘tail’ of Fam21 binding to the retromer protein Vps35. *Biochemical Journal*. 2012; 442:209–220. [PubMed: 22070227]
- Hermann GJ, Schroeder LK, Hieb CA, Kershner AM, Rabbitts BM, Fonarev P, Grant BD, Priess JR. Genetic analysis of lysosomal trafficking in *Caenorhabditis elegans*. *Molecular Biology of the Cell*. 2005; 16:3273–3288. [PubMed: 15843430]
- Huang CG, Lamitina T, Agre P, Strange K. Functional analysis of the aquaporin gene family in *Caenorhabditis elegans*. *American Journal of Physiology - Cell Physiology*. 2007; 292:C1867–C1873. [PubMed: 17229810]
- Hyenne V, Tremblay-Boudreault T, Velmurugan R, Grant BD, Loerke D, Labbé JC. RAB-5 Controls the Cortical Organization and Dynamics of PAR Proteins to Maintain *C. elegans* Early Embryonic Polarity. *PLoS ONE*. 2012; 7:e35286. [PubMed: 22545101]
- Innocenti M, Gerboth S, Rottner K, Lai FPL, Hertzog M, Stradal TEB, Frittoli E, Didry D, Polo S, Disanza A, Benesch S, Fiore PPD, Carlier MF, Scita G. Abi1 regulates the activity of N-WASP and WAVE in distinct actin-based processes. *Nat Cell Biol*. 2005; 7:969–976. [PubMed: 16155590]
- Kaksonen M, Sun Y, Drubin DG. A Pathway for Association of Receptors, Adaptors, and Actin during Endocytic Internalization. *Cell*. 2003; 115:475–487. [PubMed: 14622601]
- Kaksonen M, Toret CP, Drubin DG. Harnessing actin dynamics for clathrin-mediated endocytosis. *Nat Rev Mol Cell Biol*. 2006; 7:404–414. [PubMed: 16723976]
- Katsura T, Verbavatz JM, Farinas J, Ma T, Ausiello DA, Verkman AS, Brown D. Constitutive and regulated membrane expression of aquaporin 1 and aquaporin 2 water channels in stably transfected LLC-PK1 epithelial cells. *Proceedings of the National Academy of Sciences*. 1995; 92:7212–216.
- Kinchen JM, Cabello J, Klingele D, Wong K, Feichtinger R, Schnabel H, Schnabel R, Hengartner MO. Two pathways converge at CED-10 to mediate actin rearrangement and corpse removal in *C. elegans*. *Nature*. 2005; 434:93–99. [PubMed: 15744306]
- Legouis R, Gansmuller A, Sookhareea S, Boshier JM, Baillie DL, Labouesse M. LET-413 is a basolateral protein required for the assembly of adherens junctions in *Caenorhabditis elegans*. *Nat Cell Biol*. 2000; 2:415–422. [PubMed: 10878806]

- Leibfried A, Fricke R, Morgan MJ, Bogdan S, Bellaiche Y. *Drosophila* Cip4 and WASp Define a Branch of the Cdc42-Par6-aPKC Pathway Regulating E-Cadherin Endocytosis. *Current Biology*. 2008; 18:1639–1648. [PubMed: 18976911]
- Leung B, Hermann GJ, Priess JR. Organogenesis of the *Caenorhabditis elegans* intestine. *Dev Biol*. 1999; 216(1):114–134. [PubMed: 10588867]
- Liu J, Sun Y, Oster GF, Drubin DG. Mechanochemical crosstalk during endocytic vesicle formation. *Current Opinion in Cell Biology*. 2010; 22:36–43. [PubMed: 20022735]
- Madrid R, Le Maout S, Barrault MB, Janvier K, Benichou S, Merot J. Polarized trafficking and surface expression of the AQP4 water channel are coordinated by serial and regulated interactions with different clathrin-adaptor complexes. *EMBO J*. 2001; 20:7008–7021. [PubMed: 11742978]
- Mayle KM, Le AM, Kamei DT. The intracellular trafficking pathway of transferrin. *Biochimica et Biophysica Acta (BBA) - General Subjects*. 2012; 1820:264–281.
- Merrifield CJ, Qualmann B, Kessels MM, Almers W. Neural Wiskott Aldrich Syndrome Protein (N-WASP) and the Arp2/3 complex are recruited to sites of clathrin-mediated endocytosis in cultured fibroblasts. *European Journal of Cell Biology*. 2004; 83:13–18. [PubMed: 15085951]
- Moeller HB, Praetorius J, Rützler MR, Fenton RA. Phosphorylation of aquaporin-2 regulates its endocytosis and protein-protein interactions. *Proceedings of the National Academy of Sciences*. 2010; 107:424–429.
- Mooren OL, Galletta BJ, Cooper JA. Roles for Actin Assembly in Endocytosis. *Annual Review of Biochemistry*. 2012; 81:661–686.
- Nakayama Y, Shivas JM, Poole DS, Squirrell JM, Kulkoski JM, Schleede JB, Skop AR. Dynamin Participates in the Maintenance of Anterior Polarity in the *Caenorhabditis elegans* Embryo. *Developmental Cell*. 2009; 16:889–900. [PubMed: 19531359]
- Palamidessi A, Frittoli E, Garré M, Faretta M, Miome M, Testa I, Diaspro A, Lanzetti L, Scita G, Di Fiore PP. Endocytic Trafficking of Rac Is Required for the Spatial Restriction of Signaling in Cell Migration. *Cell*. 2008; 134:135–147. [PubMed: 18614017]
- Pan CL, Baum PD, Gu M, Jorgensen EM, Clark SG, Garriga G. C. *elegans* AP-2 and Retromer Control Wnt Signaling by Regulating MIG-14/Wntless. *Developmental Cell*. 2008; 14:132–139. [PubMed: 18160346]
- Patel FB, Bernadskaya YY, Chen E, Jobanputra A, Pooladi Z, Freeman KL, Gally C, Mohler WA, Soto MC. The WAVE/SCAR complex promotes polarized cell movements and actin enrichment in epithelia during *C. elegans* embryogenesis. *Developmental Biology*. 2008; 324:297–309. [PubMed: 18938151]
- Pollard TD. Regulation of Actin Filament Assembly by Arp2/3 Complex and Formins. *Annual Review of Biophysics and Biomolecular Structure*. 2007; 36:451–477.
- Robertson A, Smythe E, Ayscough K. Functions of actin in endocytosis. *Cellular and Molecular Life Sciences*. 2009; 66:2049–2065. [PubMed: 19290477]
- Römer W, Pontani LL, Sorre B, Rentero C, Berland L, Chambon V, Lamaze C, Bassereau P, Sykes C, Gaus K, Johannes L. Actin Dynamics Drive Membrane Reorganization and Scission in Clathrin-Independent Endocytosis. *Cell*. 2010; 140:540–553. [PubMed: 20178746]
- Saffarian S, Cocucci E, Kirchhausen T. Distinct Dynamics of Endocytic Clathrin-Coated Pits and Coated Plaques. *PLoS Biol*. 2009; 7:e1000191. [PubMed: 19809571]
- Sato M, Sato K, Fonarev P, Huang CJ, Liou W, Grant BD. *Caenorhabditis elegans* RME-6 is a novel regulator of RAB-5 at the clathrin-coated pit. *Nat Cell Biol*. 2005; 7:559–569. [PubMed: 15895077]
- Shafaq-Zadah M, Brocard L, Solari F, Michaux G. AP-1 is required for the maintenance of apico-basal polarity in the *C. elegans* intestine. *Development*. 2012; 139:2061–2070. [PubMed: 22535414]
- Shi A, Sun L, Banerjee R, Tobin M, Zhang Y, Grant BD. Regulation of endosomal clathrin and retromer-mediated endosome to Golgi retrograde transport by the J-domain protein RME-8. *EMBO J*. 2009; 28:3290–3302. [PubMed: 19763082]
- Shivas JM, Skop AR. Arp2/3 mediates early endosome dynamics necessary for the maintenance of PAR asymmetry in *Caenorhabditis elegans*. *Molecular Biology of the Cell*. 2012; 23:1917–1927. [PubMed: 22456506]

- Silva JM, Ezhkova E, Silva J, Heart S, Castillo M, Campos Y, Castro V, Bonilla F, Cordon-Cardo C, Muthuswamy SK, Powers S, Fuchs E, Hannon GJ. Cyfip1 Is a Putative Invasion Suppressor in Epithelial Cancers. *Cell*. 2009; 137:1047–1061. [PubMed: 19524508]
- Simonsen A, Lippe R, Christoforidis S, Gaullier JM, Brech A, Callaghan J, Toh BH, Murphy C, Zerial M, Stenmark H. EEA1 links PI(3)K function to Rab5 regulation of endosome fusion. *Nature*. 1998; 394:494–498. [PubMed: 9697774]
- Soto MC, Qadota H, Kasuya K, Inoue M, Tsuboi D, Mello CC, Kaibuchi K. The GEX-2 and GEX-3 proteins are required for tissue morphogenesis and cell migrations in *C. elegans*. *Genes & development*. 2002; 16:620–632. [PubMed: 11877381]
- Sun L, Liu O, Desai J, Karbassi F, Sylvain MA, Shi A, Zhou Z, Rocheleau CE, Grant BD. CED-10/Rac1 Regulates Endocytic Recycling through the RAB-5 GAP TBC-2. *PLoS Genetics*. 2012; 8:e1002785. [PubMed: 22807685]
- Taylor MJ, Perrais D, Merrifield CJ. A High Precision Survey of the Molecular Dynamics of Mammalian Clathrin-Mediated Endocytosis. *PLoS Biol*. 2011; 9:e1000604. [PubMed: 21445324]
- Toret CP, Drubin DG. The budding yeast endocytic pathway. *Journal of Cell Science*. 2006; 119:4585–4587. [PubMed: 17093262]
- Totong R, Achilleos A, Nance J. PAR-6 is required for junction formation but not apicobasal polarization in *C. elegans* embryonic epithelial cells. *Development*. 2007; 134:1259–1268. [PubMed: 17314130]
- Treusch S, Knuth S, Slaugenhaupt SA, Goldin E, Grant BD, Fares H. *Caenorhabditis elegans* functional orthologue of human protein h-mucolipin-1 is required for lysosome biogenesis. *Proceedings of the National Academy of Sciences of the United States of America*. 2004; 101:4483–4488. [PubMed: 15070744]
- Tsuboi D, Qadota H, Kasuya K, Amano M, Kaibuchi K. Isolation of the Interacting Molecules with GEX-3 by a Novel Functional Screening. *Biochemical and Biophysical Research Communications*. 2002; 292:697–701.
- Withee J, Galligan B, Hawkins N, Garriga G. *Caenorhabditis elegans* WASP and Ena/VASP Proteins Play Compensatory Roles in Morphogenesis and Neuronal Cell Migration. *Genetics*. 2004; 167:1165–1176. [PubMed: 15280232]
- Xiong H, Mohler WA, Soto MC. The branched actin nucleator Arp2/3 promotes nuclear migrations and cell polarity in the *C. elegans* zygote. *Developmental Biology*. 2011; 357:356–369. [PubMed: 21798253]
- Zhang H, Kim A, Abraham N, Khan LA, Hall DH, Fleming JT, Gobel V. Clathrin and AP-1 regulate apical polarity and lumen formation during *C. elegans* tubulogenesis. *Development*. 2012; 139:2071–2083. [PubMed: 22535410]
- Zhang Y, Grant B, Hirsh D. RME-8, a Conserved J-Domain Protein, Is Required for Endocytosis in *Caenorhabditis elegans*. *Molecular Biology of the Cell*. 2001; 12:2011–2021. [PubMed: 11451999]

1. WAVE/SCAR is the key Arp2/3 regulator for endocytosis in two *C. elegans* tissues
2. WAVE/SCAR promotes GFP::hTfR transport away from plasma membrane to early endosomes
3. WAVE/SCAR supports the subcellular enrichment of RAB-5-positive endosomes
4. Masturation of early endosomes in coelomocyte scavenger cells requires WAVE/SCAR
5. Transport through early endosomes in coelomocytes requires WAVE/SCAR

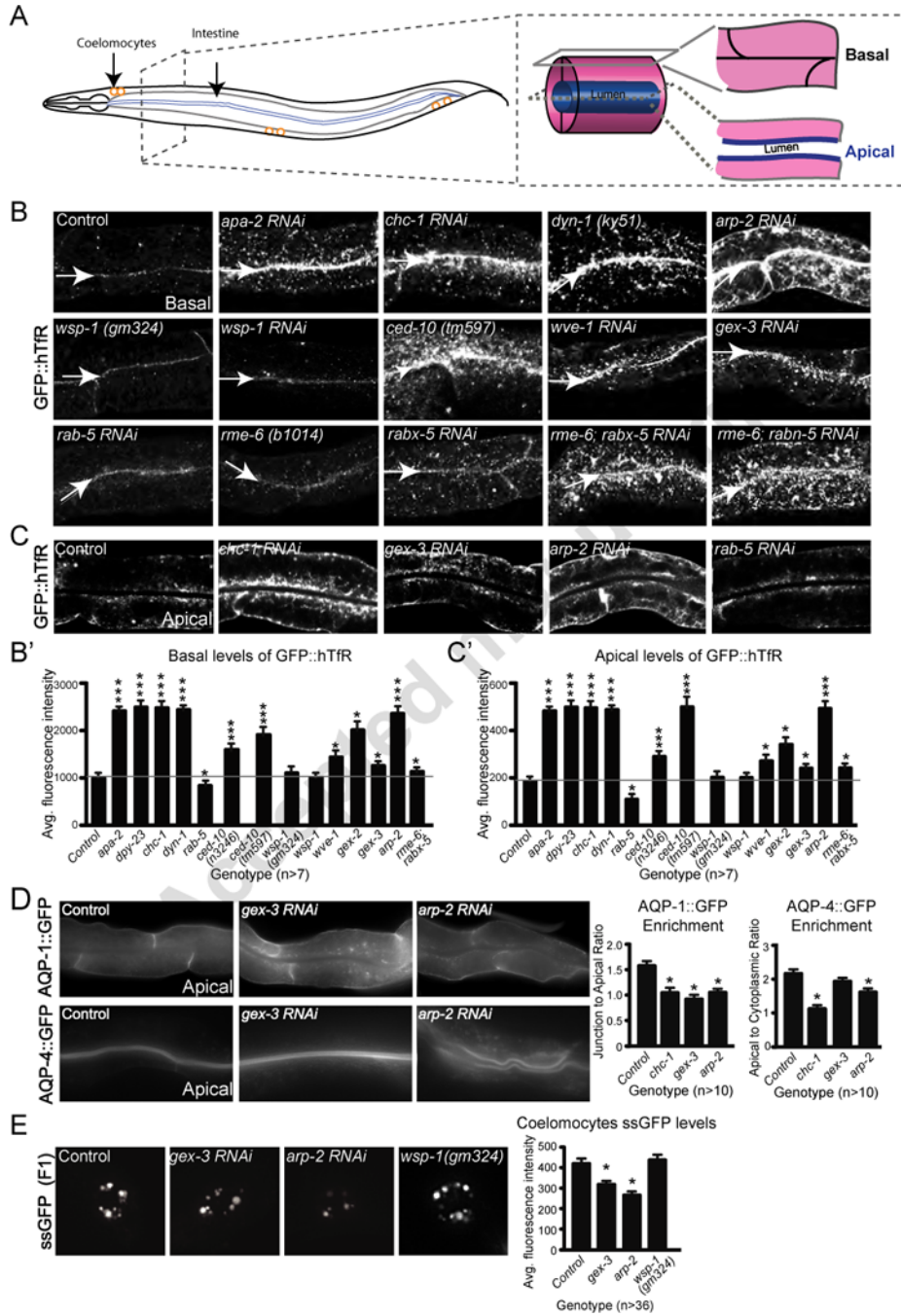


Figure 1. WAVE/SCAR regulates endocytosis in two tissues in *C. elegans*

A. The *C. elegans* adult intestine is a tube made up of only twenty cells, two per segment for most of its length. Basal/surface views are shown in panel B, while apical/center views are shown in panel C. The coelomocyte scavenger cells shown in the *myo-3::ssGFP* endocytosis assay (Fares and Greenwald, 2001) in panel E, are depicted as three pairs of orange circles.

B. Effects of WAVE/SCAR, ARP-2, Wasp and endocytic proteins on accumulation of the proposed clathrin dependent cargo, GFP::hTfR. Confocal fluorescent images of adult intestinal cells expressing hTfR tagged with GFP, basal focus. Arrows indicate the cell-cell junctions at the basal intestine. Quantification of GFP::hTfR accumulation on the basal side

is graphed in B'. For all intestinal images in this and other figures, the same anterior region of the intestine was imaged and is shown.

C. The same animals shown in panel B, apical focus, for a subset of the genotypes.

Quantification of GFP::hTfR accumulation on apical side is graphed in C.

D. *Effects of WAVE/SCAR and ARP-2 on basally and apically enriched aquaporins.*

Quantification shows changes in basal and apical distribution of AQP-1 and AQP-4, respectively, two aquaporin channels expressed in the *C. elegans* intestine (Huang et al., 2007).

E. *Effect of gex-3, arp-2 and wsp-1 on endocytosis into coelomocytes.* The *myo-3::ssGFP* endocytosis assay monitors the SEL-1 signal sequence tagged with GFP (ssGFP), produced in the muscles, as it is endocytosed by the coelomocytes. The F2 generation of synchronized L1s fed RNAi (see Methods) was imaged. The graph shows average fluorescence intensity of ssGFP in the coelomocytes (entire cell). Three independent experiments were performed with 12 animals per experiment and genotype. For this and all figures error bars show standard error of the mean (SEM) and "n" equals number of animals for each genotype.

Single asterisks indicate statistical significance, $p < 0.05$, while triple asterisks indicate $p < 0.0001$. Statistics in all figures performed with Prism software. The horizontal gray line in the large graphs of Figure 1 and 2 are drawn for ease of comparison of wild type to mutants.

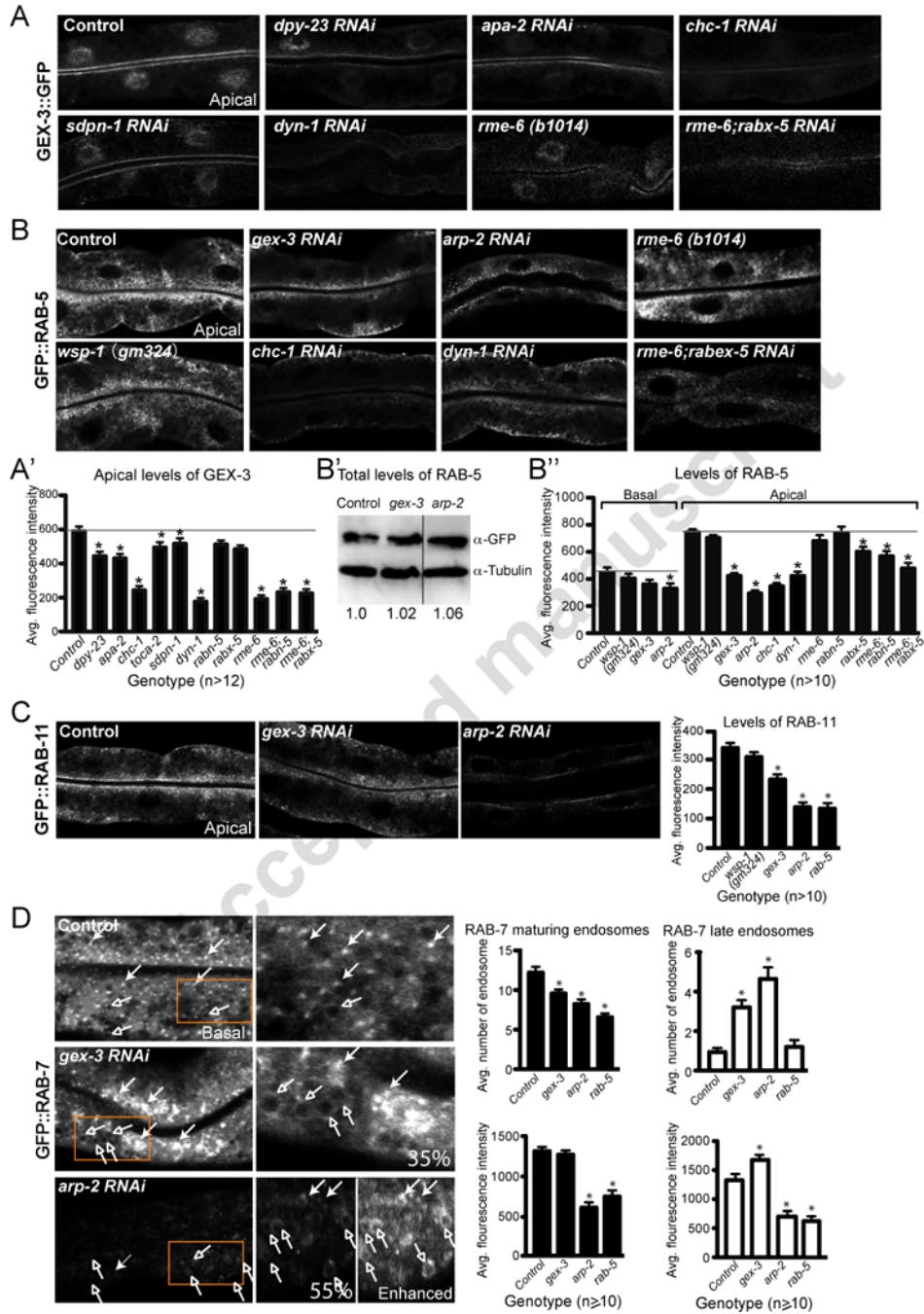


Figure 2. WAVE/SCAR complex regulates the distribution of endocytosis components
 Transgenic strains expressed in the *C. elegans* intestine were either crossed into mutant strains or fed bacteria to deplete specific genes via feeding RNAi. All images are confocal.
A. Effect of endocytosis regulators on apical enrichment of *GEX-3::GFP* at the apical intestine. The *gex-3::gfp* transgenic strain RT2287 was used. Quantification of *GEX-3::GFP* apical accumulation is shown in A'.
B. Apical and basal enrichment of *GFP::RAB-5* in animals depleted of endocytosis regulators or actin regulators. The *gfp::rab-5* transgenic strain RT327 was used. B': Western blots, with tubulin as a loading control, show levels of *GFP::RAB-5* relative to tubulin. Ratio numbers below the gels reflect the average of three gels. The *gex-3* and *arp-2* lanes

were from the same gel and joined here for ease of comparison. B^{''}: Quantification of apical and basal enrichment of GFP::RAB-5.

C. *Apical enrichment of GFP::RAB-11 in animals depleted of gex-3, arp-2, wsp-1 and rab-5.* The *gfp::rab-11* strain RT311 was used. The graph on the right shows average intensity measured at apical regions.

D. *Enrichment of GFP::RAB-7 in animals depleted of gex-3 arp-2 and rab-5.* The *gfp::rab-7* strain RT1103 was used. The closed and open arrows indicate maturing endosomes and late endosomes, respectively. The orange boxes marked in the left column are enlarged in the right column. For *arp-2*, there are two enlarged images, one shown at regular exposure, while the “Enhanced” image is over-contrasted to make structures easily visible. Percentage of animals with clumping defects is shown in the right column.

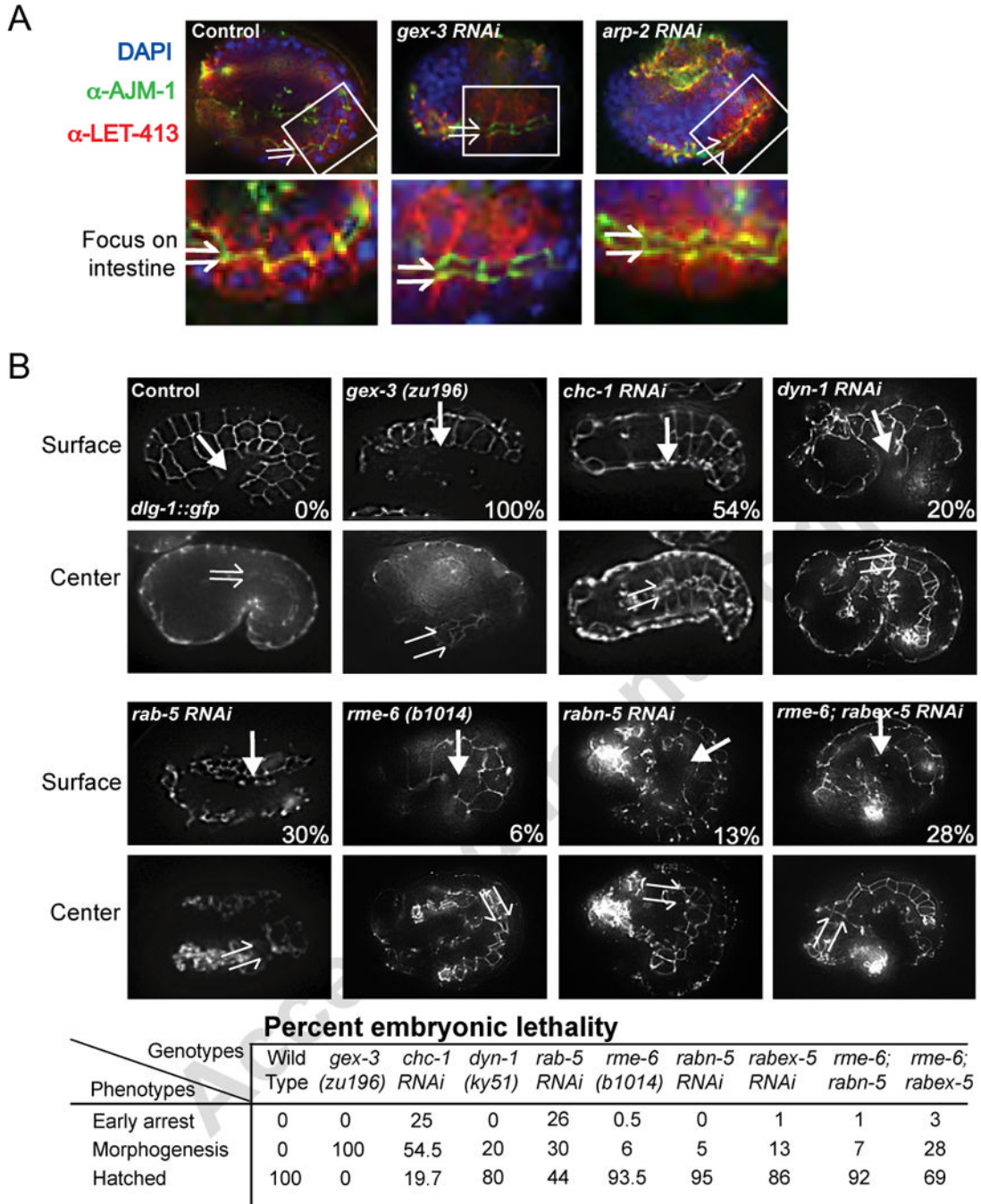


Figure 3. Endocytic molecules and WAVE/SCAR regulate morphogenesis in embryonic epithelia

A. Overall apical/basal polarity is maintained in *gex* mutants. Fixed embryos are double labeled with antibodies to AJM-1 and LET-413 to mark apical and basal domains respectively, in epithelial cells. The top panel shows the whole embryo with a white box indicating a portion of the intestinal region, which is enlarged in the bottom panel. The split arrows indicate intestinal lumen width. WT intestinal lumens are of relatively uniform narrow width, but they twist (Leung et al., 1999). *Gex* intestinal lumens progressively expand (Bernadskaya et al., 2011). Cropped regions were enhanced for contrast using the Mosaic function of iVision so that all images were enhanced equally.

B. *WAVE/SCAR and regulators of CME are required for embryonic epithelial morphogenesis.* *Top panels* - Live imaging of embryos with the *dlg-1::gfp* transgene, surface focus, allow comparison of epidermal cell migrations in wild type, WAVE/SCAR and endocytosis mutants. In wild type embryos the epidermis migrates to the ventral side of the embryo (arrow). In WAVE/SCAR and some endocytosis mutants the epidermis arrests its migration, failing to enclose the ventral surface of the embryo. *Bottom panels* - Live imaging of *dlg-1::gfp*, center focus, shows the intestinal lumen width (split arrows) in wild type, WAVE/SCAR and endocytosis mutants. The table summarizes the percent of embryos with early arrest (failures in cytokinesis or differentiation), or morphogenesis defects (fully differentiated tissues, but partial or complete failure of epidermal migration) or no defects (Hatched) for each genotype. Early arrest in some endocytosis mutants precluded scoring their morphogenesis defects, as the categories are mutually exclusive. At least 400 embryos from three independent experiments were examined. Embryos are oriented with anterior to the left and dorsal up.

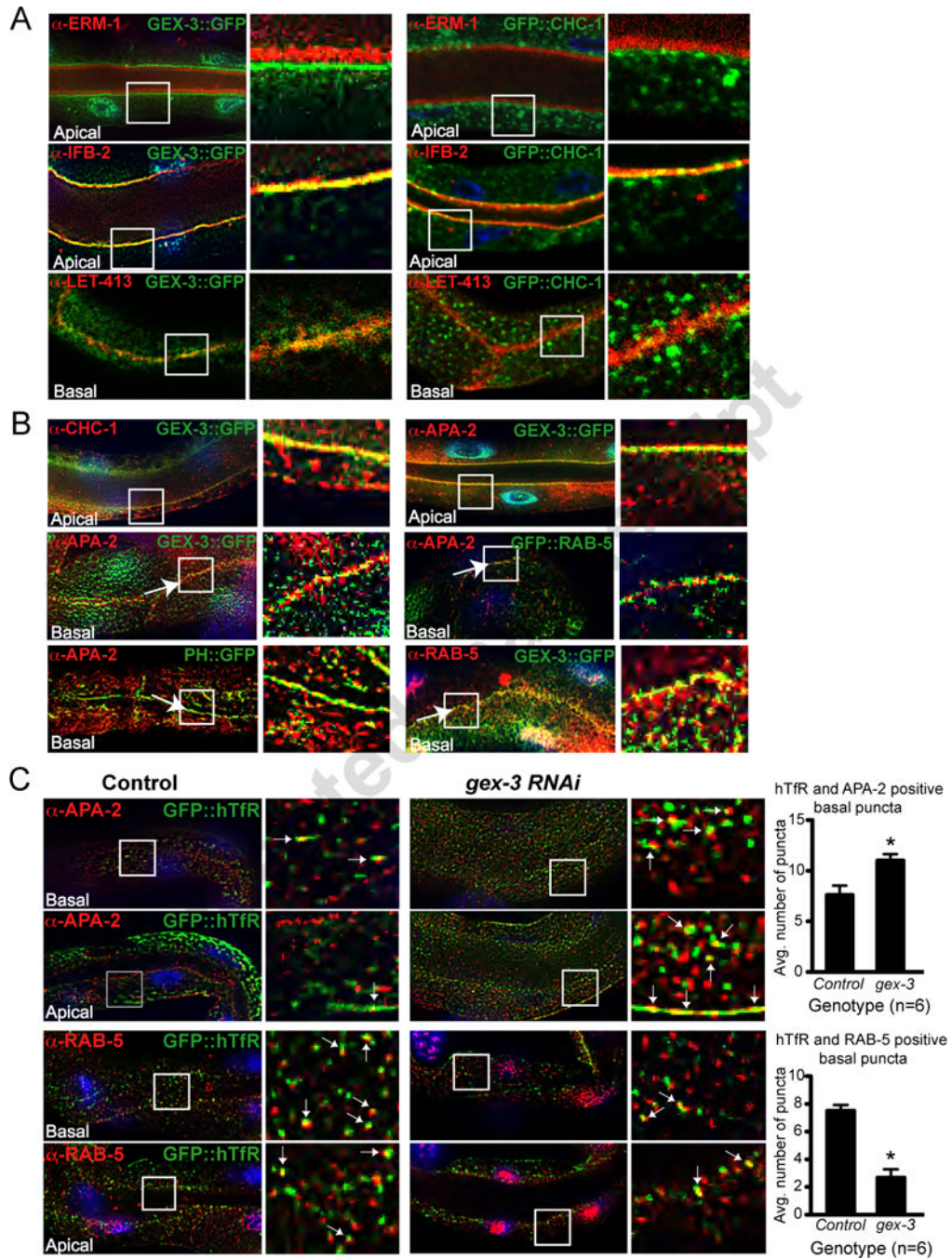


Figure 4. The WAVE/SCAR component GEX-3 localizes to similar regions as endocytosis proteins and is required for the distribution of GFP::hTfR

A. Subcellular distribution of GEX-3::GFP at apical and basal regions of the intestine.

GEX-3::GFP localization relative to apical terminal web (a-IFB-2), an apical membrane-bound protein (a-ERM-1), and the basal plasma membrane protein LET-413/Scribble. The solid white squares mark the regions enlarged on the right.

B. Subcellular distribution of GEX-3::GFP relative to regulators of CME. Relative

distribution of GFP::CHC-1, APA-2, GFP::RAB-5, GEX-3::GFP and PH::GFP. The arrows indicate the basal membrane at the junction between two intestinal cells.

C. Effect of GEX-3 on GFP::hTfR localization. The localization of GFP::hTfR is compared to that of APA-2 and RAB-5 in wild type animals and in animals depleted of GEX-3 via RNAi. White arrows indicate regions of overlap. The graphs document the number of puncta expressing both markers within a given rectangular region.

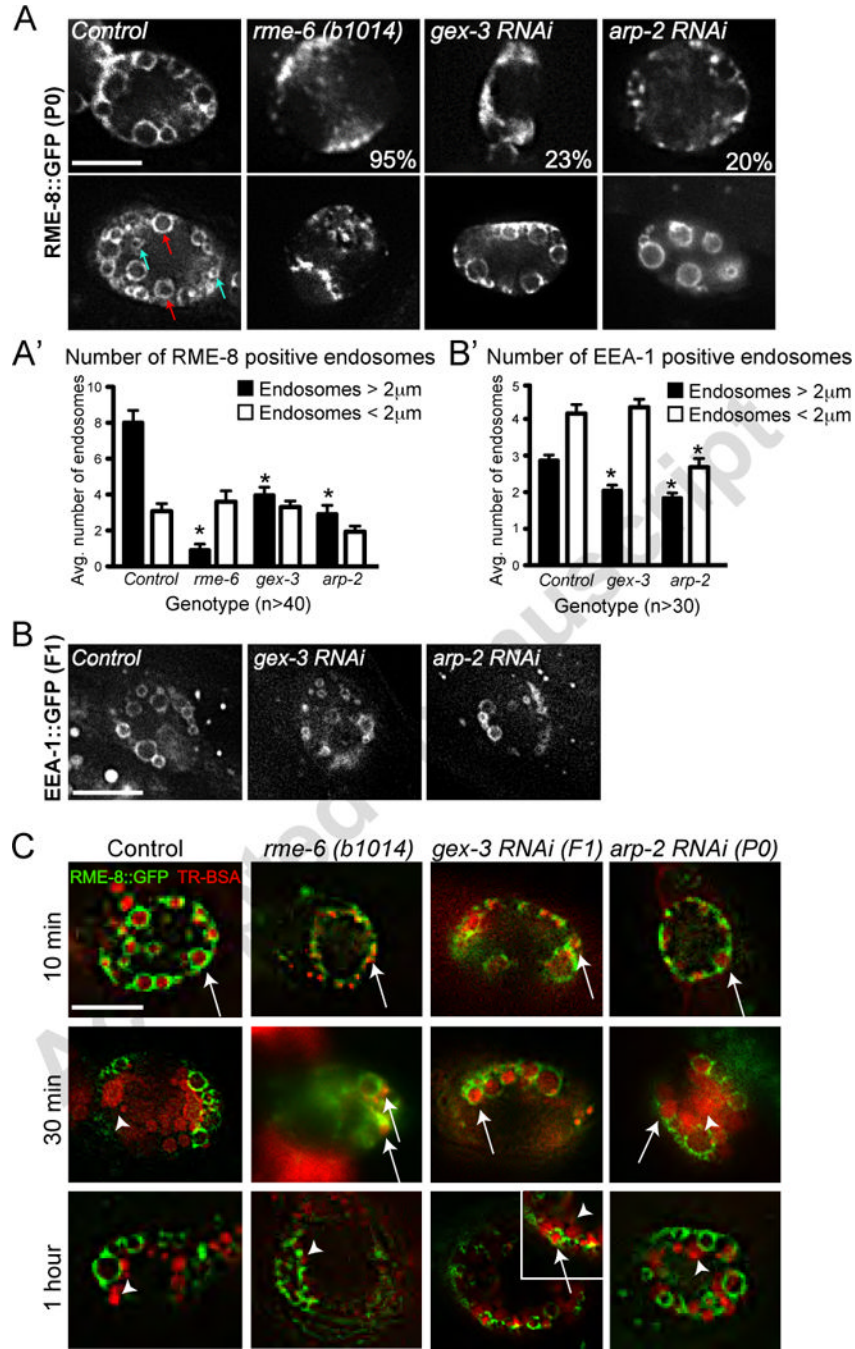


Figure 5. WAVE/SCAR and Arp2/3 are required for endosome maturation in coelomocytes
A. Effects of *gex-3* and *arp-2* on RME-8::GFP enrichment in coelomocytes. The top panels show coelomocytes with dramatically reduced RME-8::GFP-positive endosomes, similar to the effect of *rme-6* loss. Percentages indicate number of animals with the strongest endosome defects. Bottom panels show coelomocytes with less severe defects. Arrows indicate small (< 2µm, blue) and large (> 2µm, red) endosomes. **A'**: Quantitation of small and large endosomes.
B.,B' Effects of *gex-3* and *arp-2* on EEA-1::GFP enrichment in coelomocytes.
C. Effects of *gex-3* and *arp-2* on transport into and out of RME-8::GFP-positive endosomes. RME-8::GFP animals were injected with TR-BSA, in the body cavity near the head,

followed by incubation of the animals for 10, 30 and 60 minutes. Transport of TR-BSA into and out of the RME-8::GFP-positive endosomes was monitored. For comparison, the RAB-5 GEF RME-6 strongly delays transport through endosomes (Sato et al., 2005) with no accumulation in RME-8 ::GFP-positive endosomes at 30 minutes. Arrows and arrowheads indicate RME-8 positive endosomes filled with TR-BSA, and TR-BSA that has exited the endosomes, respectively. Scale bars = 10 μ m. Error bars show standard error of the mean (SEM). Asterisks indicate statistical significance, $p < 0.05$.

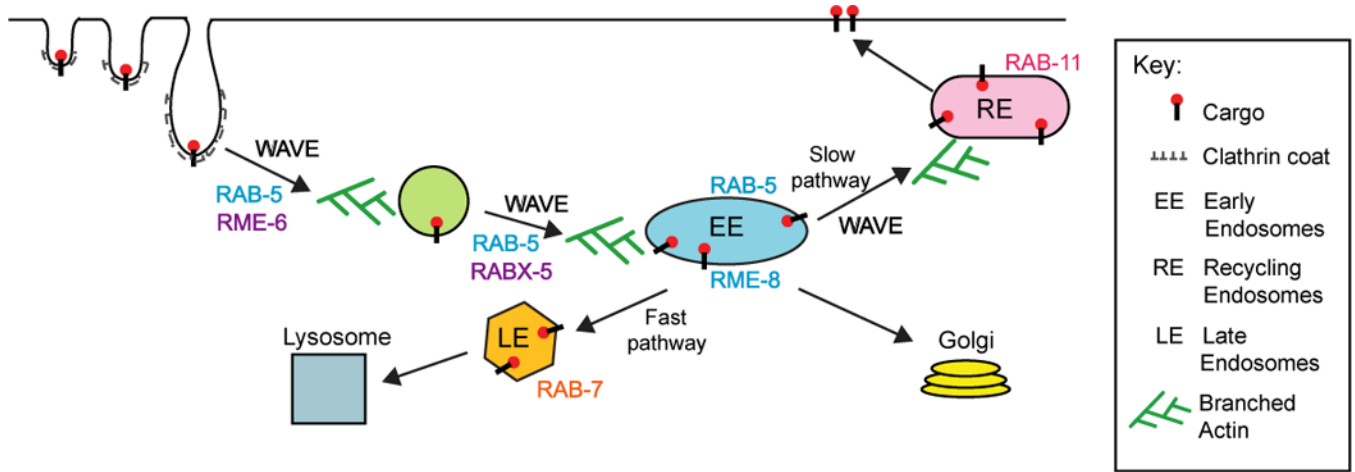


Figure 6. A model for WAVE/SCAR function during endocytosis in *C. elegans*
 We propose that Arp2/3 is essential for CME, and that one essential NPF during CME is WAVE/SCAR. WAVE/SCAR may be recruited to the plasma membrane by clathrin, F-BAR proteins like the TOCAs and/or Dynamin. WAVE/SCAR components help form a population of early endosomes enriched in RAB-5 and RME-8. Since RAB-11 enrichment is reduced by the loss of WAVE components, while RAB-7 accumulation shifts from the smaller maturing endosomes to the larger late endosomes, WAVE/SCAR may contribute to the static early endosomes (slow pathway) that has been shown to feed into the recycling endosomes in mammalian cells. Therefore WAVE/SCAR may be necessary for at least two steps in endocytosis: movement of vesicles from the plasma membrane to the early endosomes, and the maturation of a subset of early endosomes that supports endocytic recycling.